Synthetic metabolic pathways for photobiological conversion of CO_2 into hydrocarbon fuel

Ian Sofian Yunus[a], Julian Wichmann[b], Robin Wördenweber[b], Kyle J. Lauersen[b], Olaf Kruse[b] and Patrik R. Jones[a]*

[a]Department of Life Sciences, Imperial College London, SW7 2AZ London, UK

[b]Bielefeld University, Faculty of Biology, Center for Biotechnology (CeBiTec), Universitätsstrasse 27, 33615, Bielefeld, Germany.

*Corresponding author: p.jones@imperial.ac.uk

ABSTRACT

Liquid fuels sourced from fossil sources are the dominant energy form for mobile transport today. The consumption of fossil fuels is still increasing, resulting in a continued search for more sustainable methods to renew our supply of liquid fuel. Photosynthetic microorganisms naturally accumulate hydrocarbons that could serve as a replacement for fossil fuel, however productivities remain low. We report successful introduction of five synthetic metabolic pathways in two green cell factories, prokaryotic cyanobacteria and eukaryotic algae. Heterologous thioesterase expression enabled high-yield conversion of native acyl-ACP into free fatty acids (FFA) in *Synechocystis sp.* PCC 6803 but not in *Chlamydomonas reinhardtii* where the polar lipid fraction instead was enhanced. Despite no increase in measurable FFA in *Chlamydomonas*, genetic recoding and over-production of the native fatty acid photodecarboxylase (FAP) resulted in increased accumulation of 7-heptadecene. Implementation of a carboxylic acid reductase (CAR) and aldehyde deformylating oxygenase (ADO) dependent synthetic pathway in *Synechocystis* resulted in the accumulation of fatty alcohols and a decrease in the native saturated alkanes. In contrast, the replacement of CAR and ADO with *Pseudomonas mendocina* UndB (so named as it is responsible for 1-undecene biosynthesis in *Pseudomonas*) or *Chlorella variabilis* FAP resulted in high-yield conversion of thioesterase-liberated FFAs into corresponding alkenes and alkanes, respectively. At best, the engineering resulted in an increase in hydrocarbon accumulation of 8- (from 1 to 8.5 mg/g dell dry weight) and 19-fold (from 4 to 77 mg/g cell dry weight) for *Chlamydomonas* and *Synechocystis*, respectively. In conclusion, reconstitution of the eukaryotic algae pathway in the prokaryotic cyanobacteria host generated the most effective system, highlighting opportunities for mix-and-match synthetic metabolism. These studies describe functioning synthetic metabolic pathways for hydrocarbon fuel synthesis in photosynthetic microorganisms for the first time, moving us closer to the commercial implementation of photobiocatalytic systems that directly convert CO_2 into infrastructure-compatible fuels.

Keywords

Hydrocarbon fuel; Algae; Cyanobacteria; Alkanes; Alkenes; Fatty acids

Highlights

- Synthetic metabolic pathways for hydrocarbon fuels were engineered in algae
- Free fatty acids were effectively converted into alkenes and alkanes
- Transfer of algal pathway into cyanobacteria was the most effective

- Alkane yield was enhanced 19-fold in *Synechocystis spp.* PCC 6803
- Alkene yield was enhanced 8-fold in *Chlamydomonas reinhardtii*

INTRODUCTION

Cyanobacteria (prokaryotes) and algae (eukaryotes) are photosynthetic microorganisms that have evolved to naturally accumulate C15-C19 alkanes or alkenes at very low concentrations (0.02-1.12% alkane g/g cell dry weight (cdw)) (Lea-Smith et al., 2015; Schirmer et al., 2010; Sorigué et al., 2017) with the exception of naturally oleagineous species (Ajjawi et al., 2017; Metzger and Largeau, 2005; Peramuna et al., 2015). These hydrocarbons are postulated to influence the fluidity of cell membranes and are therefore essential for achieving optimal growth, indeed, the abolition of their biosynthetic capacities results in morphological defects (Lea-Smith et al., 2016). Only two enzymes, acyl-ACP reductase (AAR) and aldehyde deformylating oxygenase (ADO) are required to catalyze the bacterial conversion of acyl-ACP into alkanes (Schirmer et al., 2010). Similarly, eukaryotic microalgae also biosynthesize small quantities of alkanes and alkenes directly from fatty acids, employing the distinctly different and recently discovered fatty acid photodecarboxylase (FAP; (Sorigué et al., 2017)).

In order to engineer sustainable biotechnological systems for production of hydrocarbons for the fuel market, whether heterotrophic or light-driven, far greater yields are needed alongside other complementary non-biochemical improvements such as improved bio-process designs. Several studies have attempted to enhance alkane productivity in cyanobacteria by over-expression of the native or non-native AAR and ADO enzyme couple (Hu et al., 2013; Kageyama et al., 2015; Peramuna et al., 2015; Wang et al., 2013) which relies on acyl-ACP as the precusor. Although naturally accumulating alkane amounts have been enhanced through engineering and reported in high titres from the lipid-accumulating cyanobacteria, *Nostoc punctiforme* (up to 12.9% (g/g) cdw, (Peramuna et al., 2015)), similar efforts in the non-lipid accumulating model cyanobacterium *Synechocystis sp.* PCC 6803 (hereafter *Synechocystis* 6803) have at best yielded only 1.1% (g/g) cdw (Hu et al., 2013; Wang et al., 2013). In eukaryotic algae, the native alkene/alkane pathawy was only recently discovered and there has been no work so far to engineer the specific pathways that synthesize such hydrocarbons. Some species of algae are also known to naturally accumulate hydrocarbons that could serve as a fuel following chemical conversion. For example, certain races of the green alga *Botrococcus braunii* naturally secrete long-chain terpene hydrocarbons as a significant portion of their biomass (Eroglu and Melis, 2010; Metzger and Largeau, 2005). However, their use as a fuel source is made impossible by the incredibly slow growth rates of this alga (Cook et al., 2017). Other oleaginous algal species can accumulate a significant portion of their biomass as triacylglycerol compounds, generally under nitrogen stress. Indeed, this phenomenon drove the push for the use of algae as third generation biofuel

feedstock in the first place. However, process design and downstream processing cost considerations of large-scale algal cultivation have hindered the common adoption of algal oils for transportation fuels (Quinn and Davis, 2015). Triacylglycerol stored by eukaryotic algae can also be turned into transportation fuels via transesterification to liberate the alkanes and alkenes from the glycerol backbone. An attractive alternative to the above concepts is instead to directly secrete ready-to-use hydrocarbon products from algal cells as this would overcome issues with biomass harvesting and chemical processing and thereby greatly reduce process costs (Delrue et al., 2013).

In order to achieve such a one-step conversion of CO_2 into ready infrastructure-compatible hydrocarbons with photosynthetic hosts, however, genetic reprogramming becomes essential for introduction of synthetic metabolic pathways and optimization of the entire system. Several enzymes have recently been reported to enable biosynthesis of fatty aldehyde precursors (Akhtar et al., 2013), fatty alkanes (Bernard et al., 2012; Qiu et al., 2012), and fatty alkenes (Rude et al., 2011; Rui et al., 2015; Rui et al., 2014). Combinatorial assembly of such key enzymes into synthetic metabolic pathways consequently enabled a number of novel opportunities for hydrocarbon biosynthesis, as described by many including (Akhtar et al., 2013; Kallio et al., 2014; Sheppard et al., 2016; Zhu et al., 2017). Although such studies have so far only been reported using heterotrophic microorganisms (*Escherichia coli* and *Saccharomyces cerevisiae*) there are no reports of similar work in any phototrophic microorganism.

In this study, we describe a first and systematic study to implement synthetic metabolic pathways for the biosynthesis of hydrocarbon fuel in both prokaryotic and eukaryotic photosynthetic microorganisms using the model strains *Synechocystis* 6803 and *Chlamydomonas reinhardtii*. Several synthetic pathways towards saturated and unsaturated hydrocarbons were functionally demonstrated in *Synechocystis* 6803, increasing the hydrocarbon content up to 19-fold, and engineered *Chlamydomonas* accumulated 8-fold more alkenes than the wild-type. Interestingly, the "best" system was achieved by transferring a reconstructed pathway from eukaryotic algae into the prokaryotic cyanobacterium.

MATERIALS AND METHODS

2.1 Growth conditions, genetic constructs, transformation and screening of Escherichia coli and *Synechocystis sp.* PCC 6803

Escherichia coli DH5α was used to propagate all the plasmids used in this study. Strains were cultivated in lysogeny broth (LB) medium (LB Broth, Sigma Aldrich), 37 ^{o}C, 180 rpm, and supplemented with appropriate antibiotics (final concentration: carbenicillin 100 µg/ml, chloramphenicol 37 µg/ml, kanamycin 50 µg/ml, gentamicin 10 µg/ml, and erythromycin 200 µg/ml).

Synechocystis sp. PCC 6803, obtained from Prof. Klaas Hellingwerf (University of Amsterdam, Netherlands), was cultivated in BG11 medium without cobalt ((hereafter BG11-Co), as the metal was used as an inducer in most cultures. All media contained appropriate antibiotic(s) (final concentration: kanamycin 50 µg/ml, gentamicin 50 µg/ml, and erythromycin 20 µg/ml). Gentamicin was only used for selection on agar plates. Precultures inoculated from colonies on agar plates were grown in 6-well plates (5 ml). When the OD_{730} reached 3-4, the culture was transferred to a 100-ml Erlenmeyer flask and the OD_{730} was adjusted to 0.2 by adding BG11-Co medium to a final volume of 25 ml containing appropriate antibiotic(s). The cultivation was carried out for 10 days at 30 °C with continuous illumination at 60 µmol photons m^{-2} s^{-1} and 1% (v/v) CO_2. Each main treatment culture was induced on day 2 and samples were taken for measurement of OD_{730} and metabolites day 6 and 10. All cultivations were carried out in an AlgaeTron230 (Photon Systems Instruments) (PSI) at 30 °C with continuous illumination at 60 µmol photons m^{-2} s^{-1} and 1% (v/v) CO_2, except where noted (100-300 µmol photons m^{-2} s^{-1}). A representative growth curve and all final OD_{730} values are shown in Supplementary Figure 1.

All plasmids (Supplementary Table 1A) used for transformation of cyanobacteria were assembled using the BASIC Assembly method (Storch et al., 2015). Linkers were designed using the R20DNA software: http://www.r2odna.com/ and obtained from Integrated DNA Technologies Incorporated. The details of all linkers, primers and DNA parts used to construct each plasmid are given in Supplementary Tables 1B, 1C and 1D.

For transformation by natural assimilation, each *Synechocystis* sp. PCC 6803 strain was inoculated from freshly prepared colonies on agar plates into 25 ml BG11-Co with a starting OD 0.02. The cells were harvested when the OD_{730} reached 0.4-0.7, washed in 10 ml BG11-Co twice, and resuspended in 500 µL BG11-Co. One hundred microliters of concentrated liquid

144 culture were mixed with four to seven micrograms of plasmid and incubated at 30°C with
145 continuous illumination at 60 µmol photons m^{-2} s^{-1} and 1% (v/v) CO_2 for 12-16 h prior to
146 plating on BG11-Co agar containing 10% strength of antibiotic. To promote segregation,
147 individual colonies were restreaked on BG11-Co agar with higher antibiotic concentration. To
148 check the segregation, the biomass was resuspended in nuclease free water and exposed to
149 two freeze-thaw cycles (95°C, -80°C). Following centrifugation, 3 µL was used as a template
150 for a diagnostic polymerase chain reaction (PCR). Primers used for each PCR are listed in
151 Supplementary Table 1C. Only fully segregated mutants were used in further experiments. All
152 cyanobacteria strains used in the study are listed in Supplementary Table 2.
153 For transformation by triparental conjugation, one hundred microliters of the cargo
154 strain (*E. coli* HB101 (already carrying the pRL623 plasmid)), conjugate strain (ED8654 (Elhai
155 and Wolk, 1988)), and *Synechocystis* sp. PCC 6803 (OD_{730} ~1) were mixed and incubated for 2
156 h (30 °C, 60 µmol photons m^{-2} s^{-1}). Prior to mixing, all the *E. coli* and cyanobacteria strains
157 were washed with fresh LB and BG11-Co medium, respectively, to remove the antibiotics.
158 After 2 h of incubation, the culture mix was transferred onto BG11 agar plates without
159 antibiotic and incubated for 2 d (30 °C, 60 µmol photons m^{-2} s^{-1}). After 2 d of incubation, cells
160 were scraped from the agar plate, resuspended in 500 µL of BG11-Co medium, and
161 transferred onto a new agar plate containing 20 µg/ml erythromycin. Cells were allowed to
162 grow for one week until colonies appeared. Individual colonies were restreaked onto a new
163 plate containing 20 µg/ml erythromycin and used for subsequent experiments.
164
165 ***2.2 Growth conditions, genetic constructs, transformation and screening of***
166 ***Chlamydomonas reinhardtii***
167 *C. reinhardtii* strain UVM4 was used in this work (Neupert et al., 2009) graciously provided by
168 Prof. Dr. Ralph Bock)). The strain was routinely maintained on Tris acetate phosphate (TAP)
169 medium (Gorman and Levine, 1965) either with 1.5% agar plates or in liquid with 250 µmol
170 photons m^{-2} s^{-2}. Transformation was conducted with glass bead agitation as previously
171 described (Kindle, 1990). The amino acid sequences of *C. reinhardtii* native fatty acid
172 photodecarboxylase (FAP) (Uniprot: A8JHB7; (Sorigué et al., 2017)), *E. coli* thioesterase A
173 (TesA: P0ADA1), *Jeotgalicoccus* sp. ATCC 8456 terminal olefin-forming fatty acid
174 decarboxylase (OleTJE) (E9NSU2), and *Rhodococcus sp.* NCIMB 9784 P450 reductase RhFRED
175 (Q8KU27) were codon optimized and copies of the intron 1 of ribulose bisphosphate
176 carboxylase small subunit 2 (RBCS2) were added throughout the coding sequences as
177 previously described (Baier et al., 2018). The nucleotide sequences of optimized intron

containing genes have been submitted to NCBI, accession numbers can be found in Supplementary Table 3. All synthetic genes were chemically synthesized (GeneArt) and cloned between *Bam*HI-*Bgl*II in the pOpt2_PsaD_mVenus_Paro or pOpt2_PsaD_mRuby2_Ble vectors (Wichmann et al., 2018). PsaD represents the 36 amino acid photosystem I reaction center subunit II (PsaD) chloroplast targeting peptide (CTP) (Lauersen et al., 2015) between *Nde*I-*Bam*HI restriction sites of the pOpt2 vectors (Wichmann et al., 2018). The native FAP enzyme was designed to contain an additional glycine codon at aa position 33 to allow the insertion of a *Bam*HI site at the border of the predicted CTP. The whole synthetic enzyme including native targeting peptide was cloned *Nde*I-*Bgl*II and a version was created with the PsaD CTP built by cloning *Bam*HI-*Bgl*II into the vectors described above. Fusions of different sequences were made by digestion and complementary overhang annealing of the *Bam*HI-*Bgl*II mediated restriction sites for each respective construct as needed to obtain the fusions used in the present work (Supplementary Figure 2). After transformation, expression was confirmed by fluorescence microscopy screening for mVenus (YFP) or mRuby2 (RFP) reporters as previously described (Lauersen et al., 2016; Wichmann et al., 2018). Individual mutants were subjected to Western blotting and immuno detection to determine whether full-length protein products were formed (anti-GFP polyclonal HRP linked antibody, Thermo Fisher Scientific). Wide-field fluorescence microscopy was used to confirm chloroplast localization of YFP-linked constructs as previously described (Lauersen et al., 2016).

2.3 Product analysis

Three different extraction and analysis protocols were used for the analysis of (1) acids, (2) alcohols and (3) alkanes as well as alkenes from cyanobacteria cultures. For each analyte group, liquid cultures in flasks were mixed well by shaking prior to transferring 2 mL of liquid culture into a PYREX round bottom threaded culture tube (Corning, Manufacturer Part Number: 99449-13).

For fatty acid analysis, free fatty acid extraction was performed as described previously (Liu et al., 2011; Yunus and Jones, 2018). In brief, two hundred microliters of 1 M H_3PO_4 were added to acidify each 2 mL culture and spiked with 100 µg pentadecanoic acid (Sigma Aldrich) as an internal standard. Four millilitres of n-hexane (VWR Chemicals) was added and the mixture vortexed vigorously prior to centrifugation at 3500 x g for 3 min. The upper hexane layer was then transferred to a fresh PYREX round bottom threaded culture tube and evaporated completely under a stream of nitrogen gas. Five hundred microliters of 1.25 M HCl in methanolic solution were added to methyl esterify the free fatty acid at 85 ^{o}C for

2 h. Samples were cooled to room temperature and 500 µL of hexane was added for extraction of the fatty acid methyl esters (FAMEs).

For fatty alcohol, alkane and alkene analysis, extraction was done as described previously (Zhou et al., 2016) with modification. Briefly, 2 mL of liquid culture were spiked with 50 µg 1-nonanol, 100 µg octadecane, and 100 µg 1-pentadecanol and mixed with 4 mL of chloroform:methanol (2:1 v/v) solution. The mixture was vortexed vigorously and centrifuged at 3500 x g for 3 min. The lower organic phase was then transferred into a new glass tube and extraction was repeated one more time. The lower organic phase was combined and dried under a stream of nitrogen gas. For fatty alcohol derivatisation, the dried extract was resuspended in 100 µL chloroform, mixed with 100 µL of N, O-bistrifluoroacetamide (BSTFA) (TCI Chemicals) and transferred to an insert in a GC vial that was incubated at 60 ^{o}C for 1 h prior to GC analysis. Note that no derivatisation was needed for the analysis of hydrocarbons.

Samples (1 µL) were analysed using an Agilent Technologies (Santa Clara, CA, USA) 7890B Series Gas Chromatograph (GC) equipped with an HP-5MS column (pulsed split ratio 10:1 and split flow 10 ml/min), a 5988B Mass Spectrophotometer (MS) and a 7693 Autosampler. For the acids the GC oven program followed an initial hold at 40 ^{o}C for 3 min, a ramp at 10 ^{o}C.min^{-1} to 150 ^{o}C, a second ramp at 3 ^{o}C.min^{-1} to 270 ^{o}C, a third ramp at 30 ^{o}C.min^{-1} to 300 ^{o}C, and a final hold for 5 min. For alcohols and alkenes, there was an initial hold at 40 ^{o}C for 0.5 min, a ramp at 10 ^{o}C.min^{-1} to 300 ^{o}C, and a final hold for 4 min. For alkanes, the oven was initially held at 70 ^{o}C for 0.5 min, a ramp at 30 ^{o}C.min^{-1} to 250 ^{o}C, a second ramp at 40 ^{o}C.min^{-1} to 300 ^{o}C, and a final hold for 2 min. The acids, alkanes and alcohols were quantified by comparing the peak areas with that of the internal standards: pentadecanoate (for all acids), octadecane (for all alkanes), 1-nonanol (for C8 to C12 alcohols) and 1-pentadecanol (for C14 alcohols and above). The quantity of the main products (C15 and C17 alkanes, C15 alkene, and C12, C14, C16, and C18 alcohols and acids) were also corrected with their respective mass spectrometer response factors obtained using dilution series of commercial standards.

Gas chromatography mass spectroscopy (GC-MS) aimed at identification of hydrocarbon products from *C. reinhardtii* was conducted with solvent extracted samples following previously described protocols and internal standards (Lauersen et al., 2016). Quantification of 7-heptadecene was performed with serial dilutions (1 to 900 µM) of commercial 1-heptadecene standard (Acros Organics) in dodecane using extracted ion chromatograms with masses 55.00, 69.00, 91.00, 93.00, 83.00, 97.00, and 111.00.

RESULTS AND DISCUSSION

Several synthetic pathway designs were considered, all commencing with the liberation of "free" fatty acids from the native fatty acid biosynthesis pathway (Fig. 1), the presumed native precursor for many of the decarboxylating enzymes evaluated in this study.

3.1 Over-production of free fatty acids as precursor for hydrocarbon biosynthesis - Expression of Escherichia thioesterase deregulates lipid membrane biosynthesis in Chlamydomonas

In order to liberate FFAs in cyanobacteria we over-expressed the *E. coli* C16-C18 specific thioesterase TesA (Cho and Cronan, 1995) lacking its native signal sequence peptide ('TesA) and deleted the gene encoding the native fatty acyl ACP synthase (*aas*) (Kaczmarzyk et al., 2010; Liu et al., 2011)(Fig. 1). The native signal sequence peptide directs TesA to the periplasm in *E. coli* (Cho et al 1993) and its removal is assumed to maximize the liberation of "free" fatty acids also in cyanobacteria by retaining the enzyme in the cytosol. Such 'TesA/Δ*aas* engineering has previously been reported several times before in cyanobacteria (Liu et al., 2011, Ruffing et al., 2014; Work et al., 2015; Kato et al., 2017), with 13% (g/g cell dry weight (CDW)) as the highest reported fatty acid yield in *Synechocystis* 6803 (Liu et al 2011). Further potentially stackable modifications to the strain or process have also been reported. For example, by employing a solvent overlay, Kato et al., 2017 reported up to 36% (g/g) cdw of fatty acids excreted into the media using 'TesA/Δ*aas Synechococcus elongatus sp.* PCC 7942. In the present study, the chromosomal integration of '*tesA* into the *psbA2* site (slr1311) of *Synechocystis* 6803 Δ*aas* (Δ*aas*-'TesA), under the control of the light-inducible promoter PpsbA2S, resulted in the excretion of of C14:0 (3.5 mg/g CDW), C16:0 (23.2 mg/g CDW) and C18:0 (5.7 mg/g CDW) fatty acids with a chain-length distribution that is in agreement with previously reported findings (Liu2011) (Fig. 2A; Supplementary Fig. 3).

Overproduction of the same thioesterase ('TesA) and targeting of the enzyme product to the chloroplast was possible in *C. reinhardtii*. The synthetic algal optimized *E. coli* '*tesA* gene was fused with an N-terminal PsaD-based chloroplast targeting peptide and a C-terminal yellow fluorescent protein (YFP) encoding gene. Both the coding genes were interspersed by synthetic introns (Fig. 2B) as previously described to enhance transgene expression from the nuclear genome (Baier et al., 2018). Fluorescence microscopy indicated correct localization of the 'TesA fluorescent protein fusion to the algal chloroplast (Fig. 2C). Although no FFA could

be detected in the culture medium, a difference was observed in the lipid profile of the green algal cells, suggesting a de-regulation of fatty acid synthesis that specifically affected the polar lipid fraction of the alga. This was indicated by an over-accumulation of C18:1n9c chain lengths in the polar lipid membranes, with subtle changes observed in other acyl-ACP species such as C14:0 (Fig. 2D; Supplementary Fig. 4). Thus, 'TesA_YFP clearly had an impact on lipid metabolism in the eukaryotic algal host, but, the capture of liberated FFA by acyl-ACP or -CoA synthases is likely too effective, thereby limiting the application of the same engineering principles carried out for cyanobacteria. An annotated gene product in *Chlamydomonas* Cre06.g299800 (Phytozome v5.5) has some sequence similarity to *Synechocystis aas* and therefore represents an interesting target for future strategies to block native re-uptake of FFA in the green algal cell.

Having achieved strains with enhanced accumulation of FFA in *Synechocystis*, or at least a perturbation to the lipid biosynthetic system in *Chlamydomonas*, we proceeded to investigate enzymes that further convert FFAs into hydrocarbon end-products.

3.2 Effective conversion of free fatty acids into alkenes using UndB

Three different enzymes that catalyze the conversion of fatty acids into alkenes have been recently reported, OleT (Rude et al., 2011), UndA (Rui et al., 2014), and UndB (Rui et al., 2015) (Fig. 1). So far, the best reported productivity in both *E. coli* (Rui et al., 2015) and *S. cerevisiae* (Zhou et al., 2018) has been with UndB.

In *Synechocystis* 6803, we transformed the Δ*aas*-'TesA strain with an RSF1010-based plasmid harboring a codon-optimized *undB* under the control of the Pclac143 promoter (Markeley et al., 2014), thereby generating the strain Δ*aas*-'TesA-1010-UndB (Fig. 3A). After 10 days of cultivation, both the free fatty acids and alkanes were extracted and analyzed as described in the Materials and Methods section. The accumulation of free fatty acids was markedly reduced in the Δ*aas*-'TesA-1010-UndB strain (Fig. 3B, 3C). In its place, both 1-pentadecene and 1-heptadecene accumulated with a molar yield suggesting approximately 55% conversion of 'TesA-liberated FFAs (compare Fig. 3C with Fig. 3D). More than >84% of the FFAs disappeared relative to the Δ*aas*-'TesA strain suggesting that UndB was catalytically efficient *in vivo* and that the electrons required in the UndB reaction were fortunately supplied by an unknown source. The Δ*aas*-'TesA-1010-UndB strain displayed a lower biomass accumulation than the controls (Δ*aas*-empty and Δ*aas*–'TesA strains) (Supplementary Fig. 1), presumably due to product toxicity imparted by the alkenes. A direct comparison with the conversion efficiency in *E. coli* is not possible since the FFA conversion efficiency was not

reported in the original work (Rui et al., 2015). Despite the disappearance of C14:0 fatty acids in the Δ*aas*-'TesA-1010-UndB strain, no measurable 1-tridecene (the expected corresponding alkene) was observed in the whole culture extracts (Fig. 3C). None of the observed alkene products were secreted extracellularly (Fig. 3E).

In *Chlamydomonas*, we attempted to over-produce the *Jeotgalicoccus* sp. terminal olefin-forming fatty acid decarboxylase (OleTJE) and the *Rhodococcus sp.* P450 reductase (RhFRED). OleTJE was chosen as it could theoretically produce C17:1 and C15:0 hydrocarbons from the major lipid species of the green algal cell, C18:1 and C16:0, respectively (Fig. 1). Fusion to RhFRED has been reported to enable hydrogen peroxide-independent decarboxylase activity (Liu et al., 2014). The protein products of this decarboxylase and its fusion in either orientation to RhFRED could be detected by Western blotting and located to the algal chloroplast in fluorescence microscopy (Supplementary Figure 5). However, no differences in GC-MS profiles between the parental and expression strains could be found in either dodecane solvent overlays or cell-pellet solvent extracts.

3.3 Transfer of the CAR/ADO based pathway from E. coli to Synechocystis 6803 resulted in the accumulation of fatty alcohols and a reduction in alkane accumulation

Carboxylic acid reductases (CAR) have been previously used to construct a number of synthetic pathways for alkane biosynthesis in heterotrophic microorganisms (Akhtar et al., 2013; Kallio et al., 2014; Sheppard et al., 2016; Zhu et al., 2016). Although CAR appears to have a high capability for converting fatty acids into corresponding fatty aldehydes (Akhtar et al., 2013) (Fig. 1), a bottleneck in previous heterotrophic pathways is the subsequent conversion into alkanes by kinetically slow ADO enzymes and competition with native aldehyde reductases that more effectively convert aldehydes into alcohols (Kallio et al., 2014; Sheppard et al., 2016).

Since *Synechocystis* 6803 natively harbors an aldehyde deformylating oxygenase (ADO) with the appropriate substrate specificity (Khara et al., 2013) (Fig. 1), we first combined TesA with CAR and evaluated its ability to supply the native ADO. A synthetic operon expressing all required parts (including the CAR maturation protein Sfp) was introduced to the RSF1010 plasmid backbone (Fig. 4A) and used to transform *Synechocystis* 6803 Δ*aas*, thus creating the strain Δ*aas*-1010-TPC2. This strain accumulated both fatty acids (Fig. 4B and 4D) and fatty alcohols (Fig. 4C and 4E). The quantity of heptadecane was reduced in Δ*aas*-1010-TPC2 relative to Δ*aas*-1010-'TesA (Fig. 4F). This suggests that the introduced CAR-based pathway had not managed to increase the supply of fatty aldehydes to the native ADO. CAR and native

aldehyde reductase(s) had instead very effectively converted >90% of the FFA pool (Fig. 4D) into corresponding alcohols (Fig. 4E). The most likely reason for the increase in FFA in latter experiments is due to increased expression of 'TesA using the RSF1010 plasmid in Δ*aas*-1010-'TesA (Fig. 4D), relative to the amount of 'TesA when expressed from the chromosomal location in Δ*aas*-'TesA (Fig. 3C). Similar observations have also been previously reported by Angermayr et al. (Angermayr et al., 2014). The different promoters used in the two strains are also likely to have influenced the outcome, however, we are not aware of any studies that directly compare the two promoters head-to-head.

Substantial quantities of fatty alcohols did accumulate in the Δ*aas*-1010-TPC2 strain, suggesting that the supply of fatty aldehydes is not the limiting factor. One possibility is that the native aldehyde reductases are simply much more active than the native ADO (Eser et al., 2011; Lin et al., 2013). Another possibility is that native ADO and AAR form a close metabolon *in vivo* (Warui et al., 2015) that locks out access to ADO from external supplies of fatty aldehydes. In order to test this possibility, we attempted to create a variant of Δ*aas*-1010-TPC2 that also included chromosomal ADO over-expression casette under the PpsbA2S promoter. Despite numerous transformation and segregation attempts, however, we were unable to isolate any stable segregants. Another complementary strategy that could be considered in future work would be to eliminate native aldehyde reductases, as previously carried out in earlier *E. coli* studies (Kallio et al., 2014; Sheppard et al., 2016), although the full complement of fatty aldehyde reductase encoding genes in cyanobacteria remains unknown. Given the lack of success in producing alkanes with the CAR/ADO route in cyanobacteria we then considered alternative options for both cyanobacteria and algae.

3.4 Engineering of the native eukaryotic algae pathway and transfer to cyanobacteria results in enhanced conversion of CO_2 into alkanes

A fatty acid photodecarboxylase (FAP) that directly converts saturated and unsaturated FFAs into alkanes and alkenes, respectively, was recently discovered in eukaryotic algae (Sorigué et al., 2017). In *Chlamydomonas*, the source of free fatty acids for the native alkene pathway remains unknown, although the degradation of membrane lipids may release some FFA (illustrated in Fig. 1). However, we would expect increased accumulation of alkanes in algae if we were able to increase the cellular quantity of the native FAP and/or introduce synthetic routes to the FFA precursors.

Accordingly, we overproduced native FAP from *C. reinhardtii* (CrFAP) on its own or in combination with co-production of *E. coli* 'TesA. The over-expression of CrFAP was carried

out either with its native chloroplast targeting peptide (CTP) or the robust PsaD CTP which has been previously used to mediate chloroplast localization of numerous reporters (Lauersen et al., 2015; Lauersen et al., 2018; Rasala et al., 2013). In order to minimize any native regulation of the genomic sequence, the gene was subjected to a strategy of gene design which has recently been shown to enable robust transgene expression from the nuclear genome of this alga (Baier et al., 2018). Briefly, the sequence was codon optimized based on its amino acid sequence and multiple copies of the first intron of the *C. reinhardtii* ribulose-1,5-bisphosphate carboxylase/oxygenase (RuBisCo) small subunit 2 (rbcS2i1, NCBI: X04472.1) were spread throughout the coding sequence *in silico*. This nucleotide sequence was chemically synthesized and used for expression from the algal nuclear genome. This strategy has previously enabled heterologous overproduction of non-native sesquiterpene synthases (Lauersen et al., 2016; Lauersen et al., 2018; Wichmann et al., 2018), and in the present study also the 'TesA, OleTJE, and RhFRED proteins. However, complete codon optimization and synthetic intron spreading of a native gene has not yet been demonstrated in eukaryotic algae. Both constructs mediated full-length target protein production which was detectible in Western blots (Supplementary Fig. 5B). Replacing the native CTP with the PsaD CTP enabled more reliable and robust accumulation, which was detectible as YFP signal in the algal chloroplast (Supplementary Fig. 6) and strong bands in transformants expressing this construct in Western blots (Supplementary Fig. 5B). The parental UVM4 strain was found to contain ~0.5 mg/g 7-heptadecene as a natural product (Supplementary Fig. 7). Transformants generated with the CrFAP construct (Cr8) were found to contain up to 8x more of this alkene compared to the empty vector (Cr2) control strain (up to 8.5 ± 1.5 mg/g, Fig. 5) which was found almost exclusively within the biomass (Supplementary Fig. 7). The product was not detected in dodecane solvent overlays. CrFAP accepts a very specific substrate (*cis*-vaccenic acid, C18:1*cis*Δ11) *in vivo* (Sorigué et al., 2017), which corresponds to the accumulation of only 7-heptadecene as the only detected increased product. This substrate is an unusual FA, and is likely not naturally abundant in the algal cell. Notably, any attempts to increase the avaialability of free fatty acids using *E. coli* 'TesA did not result in any increase in the quantity or diversity of accumulated alkanes. Future enzyme engineering will likely be able to overcome this substrate specificity and increase overall yields of liberated hydrocarbons. However, a strategy which would allow secretion of these molecules, similar to the capture of heterologous terpenoids in dodecane solvent overlay (Lauersen et al., 2016; Lauersen et al., 2018; Wichmann et al., 2018), would be an attractive next target in order to enable photo-biocatalysis of hydrocarbons from the algal biomass.

Given the success with the FAP pathway in *Chlamydomonas* (present study) and earlier work in *E. coli* (Sorigué et al., 2017), as well as finding that 'TesA expression can substantially enhance the FFA pool in cyanobacteria, a synthetic FAP pathway was an obvious choice to consider also for the prokaryotic host. We therefore proceeded to implement a reconstituted variant of the eukaryotic algae pathway in cyanobacteria by combining TesA with FAP. Given the genetic instability challenges with the CAR/ADO system (see Section 3.3) we shifted our constructs to the more tightly repressed Pcoa promoter (Peca et al., 2008) for controlling the expression of *E. coli* TesA and the *Chlorella variabilis* FAP from the RSF1010 plasmid (Fig. 6A). We noted that the yield of FFA was substantially increased when driving the expression of TesA with the Pcoa promoter (Fig. 6C) compared to Pclac143 (Fig. 4D).

Despite the dominance of C16:0 fatty acids released by 'TesA in *Synechocystics* 6803, alongside minor fractions of C14:0 and C18:0, the C17:0 alkanes dominated the hydrocarbon fraction at the lower light intensity (100 μE) (Fig. 6B and 6D). This alkane profile in *Synechocystis* 6803 is very different to that observed in *E. coli* without over-expression of 'TesA (see Fig. S4 in (Sorigué et al., 2017)). We also observed substantial peaks of 8-heptadecene and 6,9-heptadecadiene, as suggested by comparison with a NIST mass spectrometry library, although a lack of standards prohibited confirmation (Supplementary Figure 8). Curiously, these alkenes were only detected at day 6 and were not present in samples harvested on day 10. As the fatty chain-length profiles differ when the same thioesterase is expressed in different *E. coli* strains (Akhtar et al., 2015; Jing et al., 2011), this suggests that the *in vivo* product profile of any thioesterase-dependent pathway also is dependent on what the fatty acid synthesis pathway provides, not just the substrate specificity of the thioesterase used.

Removal of the predicted chloroplast targeting sequence of FAP ('FAP) resulted in a doubling of the alkane yield, this time accompanied also by C15 pentadecane. As the FAP reaction is light-dependent, we also did a simple evaluation of this environmental factor. When the light intensity was tripled, the total alkane production with the Δ*aas*-1010-'TesA-'FAP strain increased to a yield of 77.1 mg/g CDW (19-fold enhancement relative to Δ*aas*) and a titer of 111.2 mg/L. The product profile also shifted (Fig. 6D) despite the lack of a similar shift in the remaining FFA fraction (Fig. 6B), suggesting that the substrate specficity of FAP is flexible and interestingly might change in response to a change in its cellular environment.

At 100 μE the introduction of 'FAP resulted in a drop in FFA accumulation of up to 90% (for C18:0), whilst for C16:0 there was only a 60% reduction (Fig. 6C). Despite repeated trials, the recovery in the measurable fatty acid to alkane conversion remained poor for C16:0

in comparison to C18:0 and the other pathways tested in *Synechocystis* 6803. This may be explained by an impact on 'TesA accumulation in the constructs also carrying the gene coding for 'FAP. Nevertheless, the reconstituted eukaryotic algae alkane pathway was more responsive to introduced modifications in the prokaryotic cyanobacterium than in its native host, though this most likely is explained by challenges associated with the release of FFA in the latter.

Although a substantial amount of both alkanes and alkenes were produced by the engineered strains, their performance likely needs to be improved before any application can be considered. Given that no genetically engineered phototrophic microalgae is currently used for commercial purposes (as far as we are aware), and LCA-studies with non-catalytic systems indicate a low predicted energy return on investment (EROI) (Carneiro et al., 2017), also other challenges with commercial algal biotechnology (e.g. contamination, bioreactor cost, energy consumption, etc) will need to be addressed.

CONCLUSIONS

The different biosynthetic systems presented in this study varied in terms of cellular context, compartmentation, promoters, operon structures and expression platforms, thus precluding a any direct comparison within and between the two species studied. However, the relative conversion efficiencies and absolute functionalities provide for a valid comparison. As such, it could be seen that the conversion of free fatty acids into alkenes by UndB and alkanes by FAP were effective (>50% conversion, for individual fatty acids up to >90% conversion), and that the native FAP pathway in *Chlamydomonas* was amenable to manipulation but that the inability to increase the FFA pool hindered further progress. Consequently, for alkanes, the reconstruction of the eukaryotic algae pathway in the prokaryotic cyanobacteria host provided a more productive system than the partially synthetic pathways in either of the prokaryotic (CAR-ADO) or eukaryotic hosts (TesA-FAP).

This work describes several approaches to employ synthetic metabolism and substantially exceed native capabilities for hydrocarbon biosynthesis in well-establised model cyanobacteria and algae. Although even greater yields have been reported in oleaginous algae and cyanobacteria that are natively endowed to accumulate lipids, the ability to introduce synthetic metabolic pathways in model strains opens up possibilities for tailored choice of both products and hosts. Importantly, the present work is based on first generation strains and further improvement is likely with systematic optimization of both strains and cultivation conditions, including the use of superior engineered or natural enzyme variants.

ACKNOWLEDGEMENTS

This project has received funding from the European Union's Horizon 2020 research and innovation programme project PHOTOFUEL under grant agreement No 640720. IY received a PhD scholarship from Indonesia Endowment Fund for Education (LPDP). The authors would also like to thank Dr. Daniel Jaeger for assistance with lipid extraction from *C. reinhardtii*.

494 **FIGURE LEGENDS**

495

496 **Figure 1. Native and synthetic metabolic pathways evaluated in the present study with**
497 **incomplete stoichiometry**. The graphic illustration shows the introduced TesA (thioesterase
498 (Cho and Cronan, 1995)), CAR (carboxylic acid reductase (Akhtar et al., 2013)), UndA
499 (responsible for 1-undecene biosynthesis in *Pseudomonas* (Rui et al., 2014)), UndB (also
500 responsible for 1-undecene biosynthesis in *Pseudomonas* (Rui et al., 2015)), OleT (responsible
501 for olefin biosynthesis in *Jeotgalicoccus* (Rude et al., 2011)) and FAP (fatty acid
502 photodecarboxylase (Sorigué et al., 2017)) enzymes alongside the native AAR/ADO (acyl-ACP
503 reductase and aldehyde deformylating oxygenase (Schirmer et al., 2010)), AHR (aldehyde
504 reductase, unknown) and FAP enzymes. Blue reactions are non-native and those in grey are
505 native. The red cross indicates deletion of the *aas* gene.

506

507 **Figure 2. Engineering for enhanced accumulation of free fatty acids.** (A) Representative
508 total ion count chromatograms for *Synechocystis* 6803 strains Δ*aas*-'TesA (black) vs. Δ*aas* only
509 (orange) extracted on day 10 of cultivation (induced day 2). Peak identities: (3) Heptadecane,
510 (4) Tetradecanoic acid, (5) Hexadecanoic acid, (6) 9,12-octadecadienoic acid, (7) 9-
511 octadecenoic acid, (8) Octadecanoic acid. (B) Graphic representation of the constructs used to
512 transform *Chlamydomonas*. CTP = Chloroplast Transit Peptide. (C) Fluorescence microscopy
513 of representative strains indicating appropriate chloroplast localization of the CTP_'TesA_YFP
514 construct. (D) Total (TL), polar (PL), and neutral (NL) gravimetric lipid fractions of
515 *Chlamydomonas* parental strain and TesA overproducing strains under nutrient replete
516 conditions (N+) and after 96 hours of nitrogen depletion (N-). PL is significantly greater in +N
517 for TesA: ttest, p:0.047 (indicated by an asterisk).

518

519 **Figure 3. Over-expression of UndB results in effective (>50%) conversion of fatty acids**
520 **into corresponding alkenes**. (A) Graphic representation of the genetic modification of
521 *Synechocystis* sp. PCC 6803 and the plasmid used for UndB expression. (B) GC-MS
522 chromatograms with extracts from the two different strains (w/wo UndB); Δ*aas*-1010-'TesA
523 (black) and Δ*aas*-1010-'TesA-UndB (orange). (C) The free fatty acid yield (relative to biomass)
524 in the whole cultures of the two strains, subdivided into the three dominant chain-lengths. (D)
525 The yield of alkenes in the whole cultures of the two strains, subdivided into the three
526 dominant chain-lengths. (E) The localization of the alkene products in whole cultures of the
527 two strains. Peak identities: (1) 1-pentadecene, (2) 1-heptadecene, (3) heptadecane, (4)

tetradecanoic acid, (5) hexadecanoic acid, (6) 9,12-octadecadienoic acid, (7) 9-octadecenoic acid, (8) octadecanoic acid. Data are mean ± SD from three biological replicates. All samples were extracted on day 10.

Figure 4. The CAR-dependent pathway produces mainly fatty alcohols. (A) Graphic overview (not to scale) illustrating the main constructs studied in the figure. (B) Total ion chromatogram from extracts of Δaas-1010-'TesA (black) and Δ*aas*-1010-TPC2 (orange). (C) Fatty alcohol profile from extracts of Δ*aas*-TPC2. The yield of fatty acids (D), alcohols (E) and alkanes (F). Peak identities: (2) 1-dodecanol, (3) heptadecane, (4) 1-tetradecanol, (5) 1-hexadecanol, (6) 9,12-octadecadien-1-ol, (7) 9-octadecen-1-ol, (8) 1-octadecanol, (9) dodecanoic acid, (10) tetradecanoic acid, (11) hexadecanoic acid, (12) octadecanoic acid. Data are mean ± SD of three biological replicates. Cultures were induced on day 2 following dilution and samples were extracted on day 10.

Figure 5. CrFAP over-expression increases 7-heptadecene yield, but heterologous thioesterase (TesA) expression, its co-expression, and C- or N-terminal fusion with CrFAP has no benefit. Mutants expressing indicated constructs (left panel) were cultivated for seven days in TAP medium with 250 µmol photons s^{-1} m^{-2} constant illumination and cell pellets were extracted with cell rupture by glass beads and dodecane for yield quantification of 7-heptadecene via GC-MS (bar graph, right). All constructs bear a PsaD chloroplast targeting peptide (CTP) to allow protein transit to the chloroplast. Arrows and plus sign indicate co-expression in double transformed mutants. Error bars represent 95% confidence intervals of single strains cultivated in biological triplicates.

Figure 6. **Conversion of free fatty acids into alkanes in cyanobacteria using FAP**. (A) Graphic representative of the plasmids used to transform *Synechocystis* sp. PCC 6803. (B) Total ion chromatogram from Δ*aas*-Pcoa-'TesA (left) and Δ*aas*-1010-Pcoa-'TesA-'FAP (100 mE, middle; 300 mE, right). The free fatty acid (C) and alkane (D) yield in all tested strains. Data are mean ± SD of three biological replicates. Samples were extracted on day 10. Peak: (1) heptadecane, (2) octadecane (internal standard), (3) pentadecane, (4) undecane, (5) tridecane, (6) hexadecanoic acid.

562 **REFERENCES**

563 Ajjawi, I., Verruto, J., Aqui, M., Soriaga, L. B., Coppersmith, J., Kwok, K., Peach, L., Orchard, E.,
564 Kalb, R., Xu, W., Carlson, T. J., Francis, K., Konigsfeld, K., Bartalis, J., Schultz, A., Lambert,
565 W., Schwartz, A. S., Brown, R., Moellering, E. R., 2017. Lipid production in
566 Nannochloropsis gaditana is doubled by decreasing expression of a single
567 transcriptional regulator. Nat Biotechnol. 35**,** 647-652.
568 Akhtar, M. K., Dandapani, H., Thiel, K., Jones, P. R., 2015. Microbial production of 1-octanol - a
569 naturally excreted biofuel with diesel-like properties. Metabolic Engineering
570 Communications. 2**,** 1-5.
571 Akhtar, M. K., Turner, N. J., Jones, P. R., 2013. Carboxylic acid reductase is a versatile enzyme
572 for the conversion of fatty acids into fuels and chemical commodities. Proc Natl Acad
573 Sci U S A. 110**,** 87-92.
574 Angermayr, S. A., van der Woude, A. D., Correddu, D., Vreugdenhil, A., Verrone, V., Hellingwerf,
575 K. J., 2014. Exploring metabolic engineering design principles for the photosynthetic
576 production of lactic acid by Synechocystis sp. PCC6803. Biotechnol Biofuels. 7**,** 99.
577 Baier, T., Wichmann, J., Kruse, O., Lauersen, K. J., 2018. Intron-containing algal transgenes
578 mediate efficient recombinant gene expression in the green microalga Chlamydomonas
579 reinhardtii. Nucleic Acids Research. gky532-gky532.
580 Bernard, A., Domergue, F., Pascal, S., Jetter, R., Renne, C., Faure, J. D., Haslam, R. P., Napier, J. A.,
581 Lessire, R., Joubès, J., 2012. Reconstitution of Plant Alkane Biosynthesis in Yeast
582 Demonstrates That Arabidopsis ECERIFERUM1 and ECERIFERUM3 Are Core
583 Components of a Very-Long-Chain Alkane Synthesis Complex. Plant Cell. 24**,** 3106-18.
584 Carneiro, M. L. N. M., Pradelle, F., Braga, S. L., Gomes, M. S. P., Martins, A. R. F. A., Turkovics, F.,
585 Pradelle, R. N. C., 2017. Potential of biofuels from algae: Comparison with fossil fuels,
586 ethanol and biodiesel in Europe and Brazil through life cycle assessment (LCA).
587 Renewable and Sustainable Energy Reviews. 73**,** 632-653.
588 Cho, H., Cronan, J. E., 1995. Defective export of a periplasmic enzyme disrupts regulation of
589 fatty acid synthesis. J Biol Chem. 270**,** 4216-9.
590 Cook, C., Dayananda, C., Tennant Richard, K., Love, J., 2017. Third‐Generation Biofuels from
591 the Microalga, Botryococcus braunii. Biofuels and Bioenergy.
592 Delrue, F., Li-Beisson, Y., Setier, P. A., Sahut, C., Roubaud, A., Froment, A. K., Peltier, G., 2013.
593 Comparison of various microalgae liquid biofuel production pathways based on
594 energetic, economic and environmental criteria. Bioresour Technol. 136C**,** 205-212.

595 Elhai, J., Wolk, C. P., 1988. Conjugal transfer of DNA to cyanobacteria. Methods Enzymol. 167,
596 747-54.
597 Eroglu, E., Melis, A., 2010. Extracellular terpenoid hydrocarbon extraction and quantitation
598 from the green microalgae Botryococcus braunii var. Showa. Bioresource Technology.
599 101, 2359-2366.
600 Eser, B. E., Das, D., Han, J., Jones, P. R., Marsh, E. N., 2011. Oxygen-independent alkane
601 formation by non-heme iron-dependent cyanobacterial aldehyde decarbonylase:
602 investigation of kinetics and requirement for an external electron donor. Biochemistry.
603 50, 10743-50.
604 Gorman, D. S., Levine, R. P., 1965. Cytochrome f and plastocyanin: their sequence in the
605 photosynthetic electron transport chain of Chlamydomonas reinhardi. Proc Natl Acad
606 Sci U S A. 54, 1665-9.
607 Hu, P., Borglin, S., Kamennaya, N. A., Chen, L., Park, H., Mahoney, L., Kijac, A., Shan, G.,
608 Chavarría, K. L., Zhang, C., Quinn, N. W. T., Wemmer, D., Holman, H.-Y., Jansson, C., 2013.
609 Metabolic phenotyping of the cyanobacterium Synechocystis 6803 engineered for
610 production of alkanes and free fatty acids. Applied Energy. 102, 850-859.
611 Jing, F., Cantu, D. C., Tvaruzkova, J., Chipman, J. P., Nikolau, B. J., Yandeau-Nelson, M. D., Reilly,
612 P. J., 2011. Phylogenetic and experimental characterization of an acyl-ACP thioesterase
613 family reveals significant diversity in enzymatic specificity and activity. BMC Biochem.
614 12, 44.
615 Kaczmarzyk, D., Cengic, I., Yao, L., Hudson, E.P., 2018. Diversion of the long-chain acyl- ACP
616 pool in Synechocystis to fatty alcohols through CRISPRi repression of the es- sential
617 phosphate acyltransferase PlsX. Metab. Eng. 45, 59–66.
618 Kageyama, H., Waditee-Sirisattha, R., Sirisattha, S., Tanaka, Y., Mahakhant, A., Takabe, T., 2015.
619 Improved Alkane Production in Nitrogen-Fixing and Halotolerant Cyanobacteria via
620 Abiotic Stresses and Genetic Manipulation of Alkane Synthetic Genes. Curr Microbiol.
621 71, 115-20.
622 Kallio, P., Pasztor, A., Thiel, K., Akhtar, M. K., Jones, P. R., 2014. An engineered pathway for the
623 biosynthesis of renewable propane. Nature Communications. 5:4731.
624 Kato, A., Takatani, N., Ikeda, K., Maeda, S.I., Omata, T., 2017. Removal of the product from the
625 culture medium strongly enhances free fatty acid production by genetically
626 engineered. Biotechnol. Biofuels 10, 141.

627 Khara, B., et al., 2013. Production of propane and other short-chain alkanes by structure-
628 based engineering of ligand specificity in aldehyde-deformylating oxygenase.
629 ChemBioChem 14, 1204–1208.
630 Kindle, K. L., 1990. High-frequency nuclear transformation of Chlamydomonas reinhardtii.
631 Proc Natl Acad Sci U S A. 87**,** 1228-32.
632 Lauersen, K. J., Baier, T., Wichmann, J., Wördenweber, R., Mussgnug, J. H., Hübner, W., Huser,
633 T., Kruse, O., 2016. Efficient phototrophic production of a high-value sesquiterpenoid
634 from the eukaryotic microalga Chlamydomonas reinhardtii. Metab Eng. 38**,** 331-343.
635 Lauersen, K. J., Kruse, O., Mussgnug, J. H., 2015. Targeted expression of nuclear transgenes in
636 Chlamydomonas reinhardtii with a versatile, modular vector toolkit. Appl Microbiol
637 Biotechnol. 99**,** 3491-503.
638 Lauersen, K. J., Wichmann, J., Baier, T., Kampranis, S. C., Pateraki, I., Møller, B. L., Kruse, O.,
639 2018. Phototrophic production of heterologous diterpenoids and a hydroxy-
640 functionalized derivative from Chlamydomonas reinhardtii. Metabolic Engineering.
641 Lea-Smith, D. J., Biller, S. J., Davey, M. P., Cotton, C. A., Perez Sepulveda, B. M., Turchyn, A. V.,
642 Scanlan, D. J., Smith, A. G., Chisholm, S. W., Howe, C. J., 2015. Contribution of
643 cyanobacterial alkane production to the ocean hydrocarbon cycle. Proc Natl Acad Sci U
644 S A. 112**,** 13591-6.
645 Lea-Smith, D. J., Ortiz-Suarez, M. L., Lenn, T., Nürnberg, D. J., Baers, L. L., Davey, M. P., Parolini,
646 L., Huber, R. G., Cotton, C. A., Mastroianni, G., Bombelli, P., Ungerer, P., Stevens, T. J.,
647 Smith, A. G., Bond, P. J., Mullineaux, C. W., Howe, C. J., 2016. Hydrocarbons Are Essential
648 for Optimal Cell Size, Division, and Growth of Cyanobacteria. Plant Physiol. 172**,** 1928-
649 1940.
650 Lin, F., Das, D., Lin, X. N., Marsh, E. N., 2013. Aldehyde-forming fatty acyl-CoA reductase from
651 cyanobacteria: expression, purification and characterization of the recombinant
652 enzyme. FEBS J. 280**,** 4773-81.
653 Liu, X., Sheng, J., Curtiss, R., 2011. Fatty acid production in genetically modified cya-
654 nobacteria. Proc. Natl. Acad. Sci. USA 108, 6899–6904.
655 Liu, Y., Wang, C., Yan, J., Zhang, W., Guan, W., Lu, X., Li, S., 2014. Hydrogen peroxide-
656 independent production of α-alkenes by OleTJE P450 fatty acid decarboxylase.
657 Biotechnol Biofuels. 7**,** 28.
658 Markley, A.L., Begemann, M.B., Clarke, R.E., Gordon, G.C., Pfleger, B.F, 2015. . A syn- thetic
659 biology toolbox for controlling gene expression in the cyanobacterium Synechococcus
660 sp. PCC 7002. ACS Synth. Biol. 4, 595–603.

661 Metzger, P., Largeau, C., 2005. Botryococcus braunii: a rich source for hydrocarbons and
662 related ether lipids. Appl Microbiol Biotechnol. 66**,** 486-96.
663 Neupert, J., Karcher, D., Bock, R., 2009. Generation of Chlamydomonas strains that efficiently
664 express nuclear transgenes. Plant J. 57**,** 1140-50.
665 Peca, L., Kós, P. B., Máté, Z., Farsang, A., Vass, I., 2008. Construction of bioluminescent
666 cyanobacterial reporter strains for detection of nickel, cobalt and zinc. FEMS Microbiol
667 Lett. 289**,** 258-64.
668 Peramuna, A., Morton, R., Summers, M. L., 2015. Enhancing alkane production in
669 cyanobacterial lipid droplets: a model platform for industrially relevant compound
670 production. Life (Basel). 5**,** 1111-26.
671 Qiu, Y., Tittiger, C., Wicker-Thomas, C., Le Goff, G., Young, S., Wajnberg, E., Fricaux, T., Taquet,
672 N., Blomquist, G. J., Feyereisen, R., 2012. An insect-specific P450 oxidative
673 decarbonylase for cuticular hydrocarbon biosynthesis. Proc Natl Acad Sci U S A.
674 Quinn, J. C., Davis, R., 2015. The potentials and challenges of algae based biofuels: a review of
675 the techno-economic, life cycle, and resource assessment modeling. Bioresour Technol.
676 184**,** 444-452.
677 Rasala, B. A., Barrera, D. J., Ng, J., Plucinak, T. M., Rosenberg, J. N., Weeks, D. P., Oyler, G. A.,
678 Peterson, T. C., Haerizadeh, F., Mayfield, S. P., 2013. Expanding the spectral palette of
679 fluorescent proteins for the green microalga Chlamydomonas reinhardtii. Plant J. 74**,**
680 545-56.
681 Rude, M. A., Baron, T. S., Brubaker, S., Alibhai, M., Del Cardayre, S. B., Schirmer, A., 2011.
682 Terminal olefin (1-alkene) biosynthesis by a novel p450 fatty acid decarboxylase from
683 Jeotgalicoccus species. Appl Environ Microbiol. 77**,** 1718-27.
684 Ruffing, A.M., 2014. Improved free fatty acid production in cyanobacteria with Synechococcus
685 sp. PCC 7002 as host. Front. Bioeng. Biotechnol. 2, 17.
686 Rui, Z., Harris, N. C., Zhu, X., Huang, W., Zhang, W., 2015. Discovery of a Family of Desaturase-
687 Like Enzymes for 1-Alkene Biosynthesis. ACS Catalysis. 5**,** 7091-7094.
688 Rui, Z., Li, X., Zhu, X., Liu, J., Domigan, B., Barr, I., Cate, J. H., Zhang, W., 2014. Microbial
689 biosynthesis of medium-chain 1-alkenes by a nonheme iron oxidase. Proc Natl Acad Sci
690 U S A. 111**,** 18237-42.
691 Schirmer, A., Rude, M., Li, X., Popova, E., del Cardayre, S., 2010. Microbial biosynthesis of
692 alkanes. Science. 329**,** 559-62.
693 Sheppard, M. J., Kunjapur, A. M., Prather, K. L. J., 2016. Modular and selective biosynthesis of
694 gasoline-range alkanes. Metab Eng. 33**,** 28-40.

695 Sorigué, D., Légeret, B., Cuiné, S., Blangy, S., Moulin, S., Billon, E., Richaud, P., Brugière, S.,
696 Couté, Y., Nurizzo, D., Müller, P., Brettel, K., Pignol, D., Arnoux, P., Li-Beisson, Y., Peltier,
697 G., Beisson, F., 2017. An algal photoenzyme converts fatty acids to hydrocarbons.
698 Science. 357**,** 903-907.
699 Storch, M., Casini, A., Mackrow, B., Fleming, T., Trewhitt, H., Ellis, T., Baldwin, G. S., 2015.
700 BASIC: A New Biopart Assembly Standard for Idempotent Cloning Provides Accurate,
701 Single-Tier DNA Assembly for Synthetic Biology. ACS Synth Biol. 4**,** 781-7.
702 Wang, W., Liu, X., Lu, X., 2013. Engineering cyanobacteria to improve photosynthetic
703 production of alka(e)nes. Biotechnol Biofuels. 6**,** 69.
704 Warui, D. M., Pandelia, M. E., Rajakovich, L. J., Krebs, C., Bollinger, J. M., Booker, S. J., 2015.
705 Efficient delivery of long-chain fatty aldehydes from the Nostoc punctiforme acyl-acyl
706 carrier protein reductase to its cognate aldehyde-deformylating oxygenase.
707 Biochemistry. 54**,** 1006-15.
708 Wichmann, J., Baier, T., Wentnagel, E., Lauersen, K. J., Kruse, O., 2018. Tailored carbon
709 partitioning for phototrophic production of (E)-α-bisabolene from the green microalga
710 Chlamydomonas reinhardtii. Metab Eng. 45**,** 211-222.
711 Work, V.H., Melnicki, M.R., Hill, E.A., Davies, F.K., Kucek, L.A., Beliaev, A.S., et al., 2015. Lauric
712 acid production in a glycogen-less strain of Synechococcus sp. PCC 7002. Front Bioeng.
713 Biotechnol. 3.
714 Yunus, I.Y., Jones, P.R., 2018. Photosynthesis-dependent biosynthesis of medium chain-length
715 fatty acids and alcohols. Metab Eng. 49, 59-68.
716 Zhou, Y. J., Hu, Y., Zhu, Z., Siewers, V., Nielsen, J., 2018. Engineering 1-Alkene Biosynthesis and
717 Secretion by Dynamic Regulation in Yeast. ACS Synth Biol. 7**,** 584-590.
718 Zhu, Z., Zhou, Y. J., Kang, M. K., Krivoruchko, A., Buijs, N. A., Nielsen, J., 2017. Enabling the
719 synthesis of medium chain alkanes and 1-alkenes in yeast. Metab Eng. 44**,** 81-88.
720

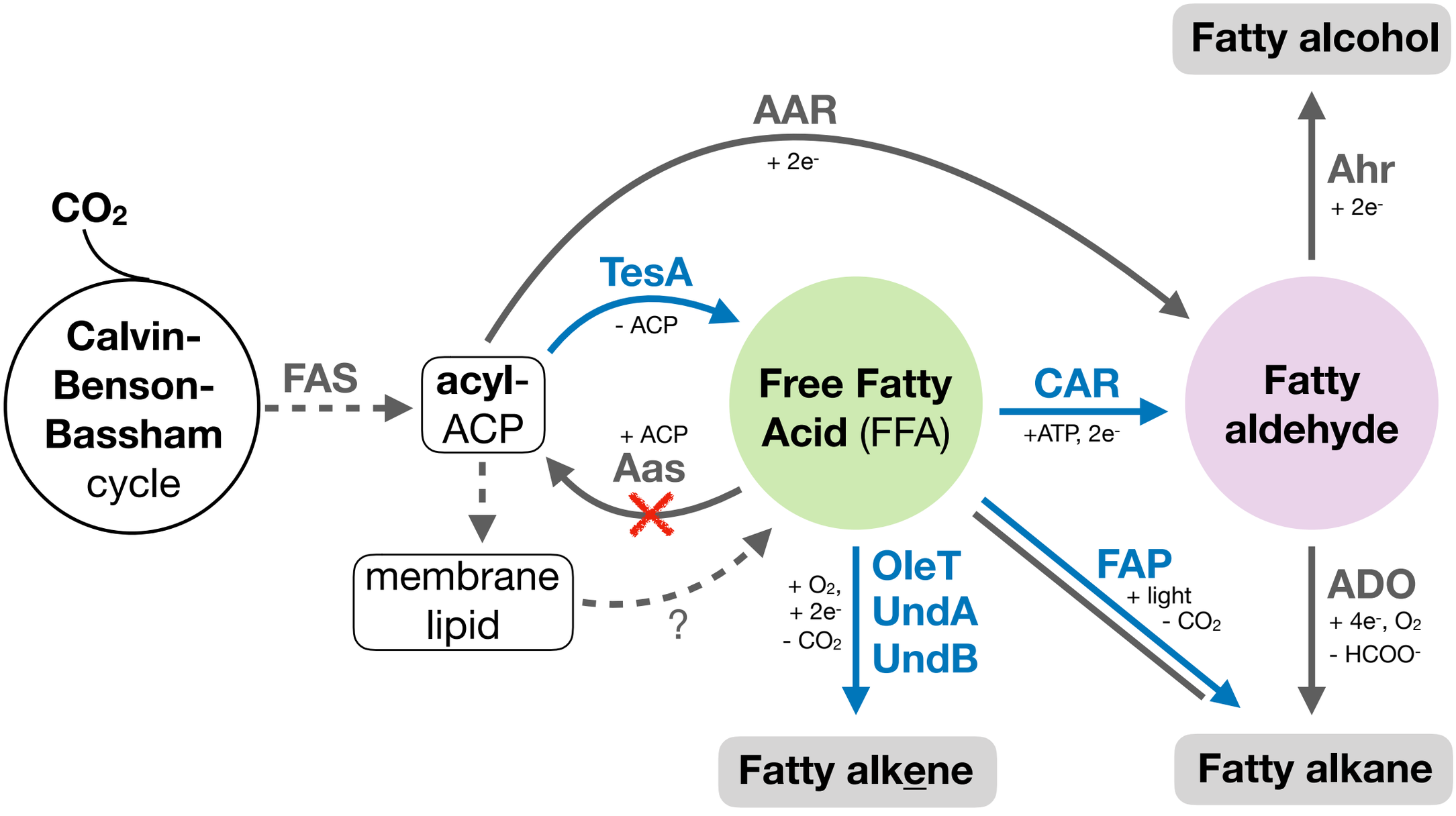
Fatty alcohol
AAR
+ 2e-
Ahr
+ 2e-
CO2
Calvin-Benson-Bassham cycle
FAS
acyl-ACP
TesA
- ACP
+ ACP
Aas
Free Fatty Acid (FFA)
CAR
+ATP, 2e-
Fatty aldehyde
membrane lipid
?
+ O2, + 2e- - CO2
OleT
UndA
UndB
FAP
+ light
- CO2
ADO
+ 4e-, O2
- HCOO-
Fatty alkene
Fatty alkane

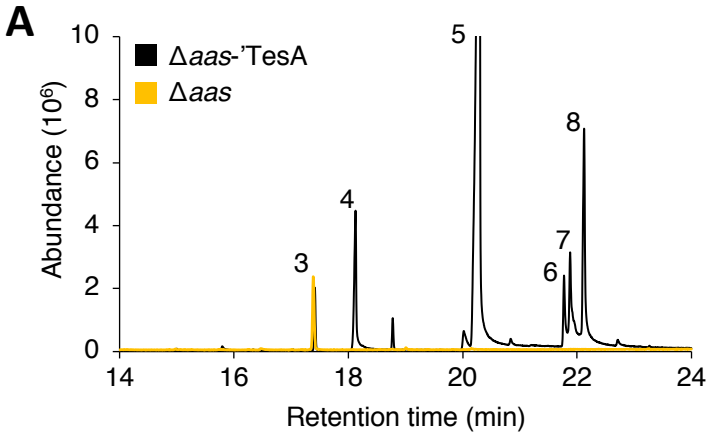
A
Δaas-'TesA
Δaas
Abundance (10^6)
Retention time (min)
3
4
5
6
7
8

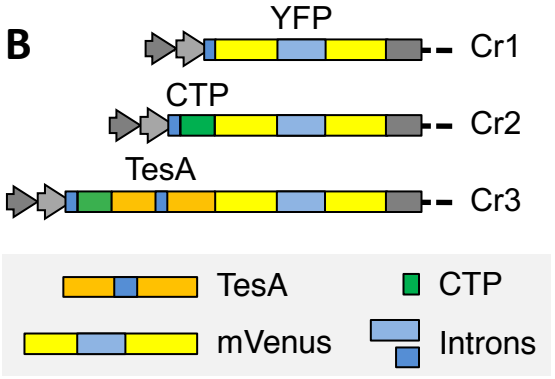
B
YFP
Cr1
CTP
Cr2
TesA
Cr3
TesA
CTP
mVenus
Introns

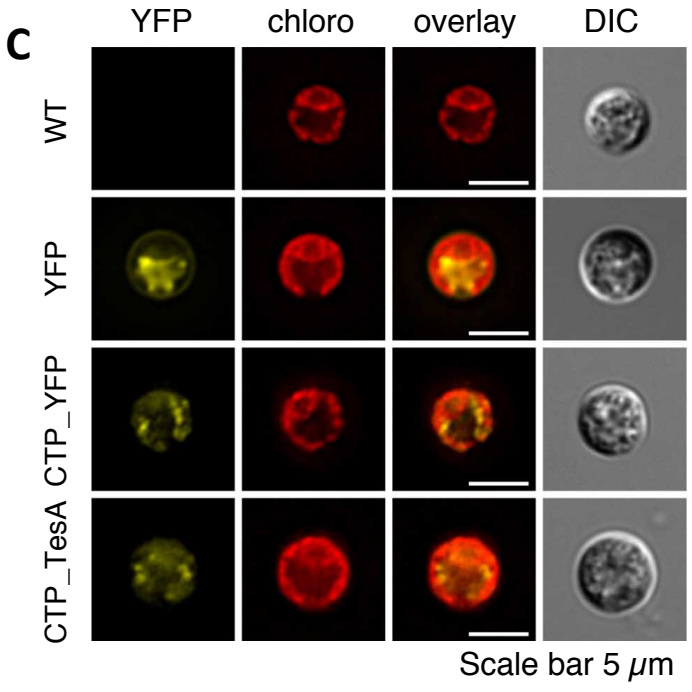
C
YFP
chloro
overlay
DIC
WT
YFP
CTP_YFP
CTP_TesA
Scale bar 5 μm

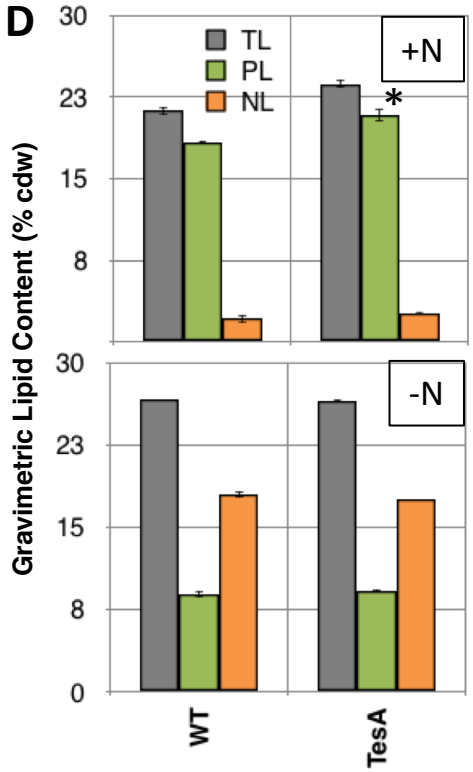
D
TL
PL
NL
+N
-N
*
Gravimetric Lipid Content (% cdw)
WT
TesA

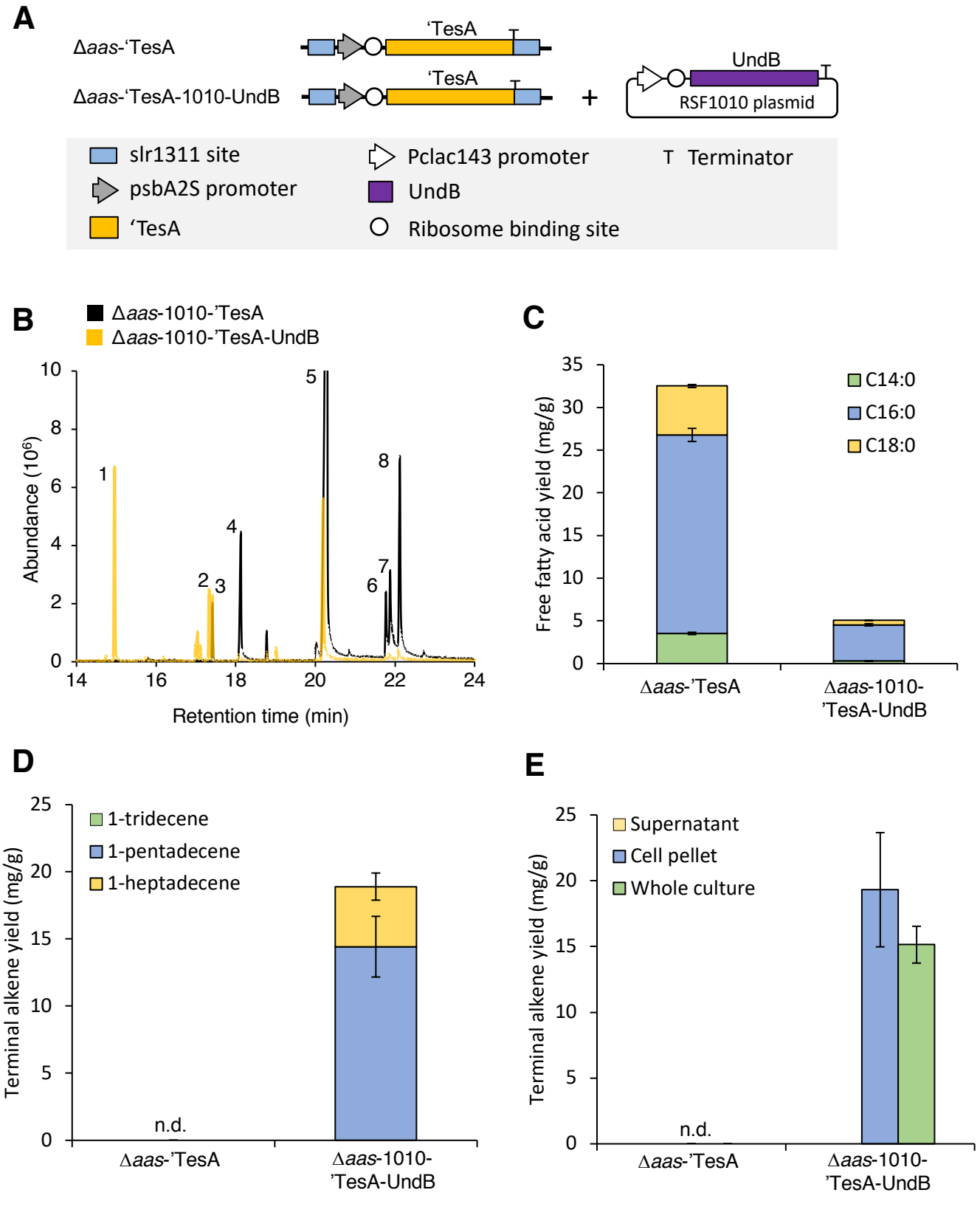
A
Δaas-'TesA
'TesA
Δaas-'TesA-1010-UndB
'TesA
+
UndB
RSF1010 plasmid
slr1311 site
psbA2S promoter
'TesA
Pclac143 promoter
UndB
Ribosome binding site
T Terminator
B
Δaas-1010-'TesA
Δaas-1010-'TesA-UndB
Abundance (10^6)
Retention time (min)
1
2
3
4
5
6
7
8
C
Free fatty acid yield (mg/g)
C14:0
C16:0
C18:0
Δaas-'TesA
Δaas-1010-'TesA-UndB
D
Terminal alkene yield (mg/g)
1-tridecene
1-pentadecene
1-heptadecene
n.d.
Δaas-'TesA
Δaas-1010-'TesA-UndB
E
Terminal alkene yield (mg/g)
Supernatant
Cell pellet
Whole culture
n.d.
Δaas-'TesA
Δaas-1010-'TesA-UndB

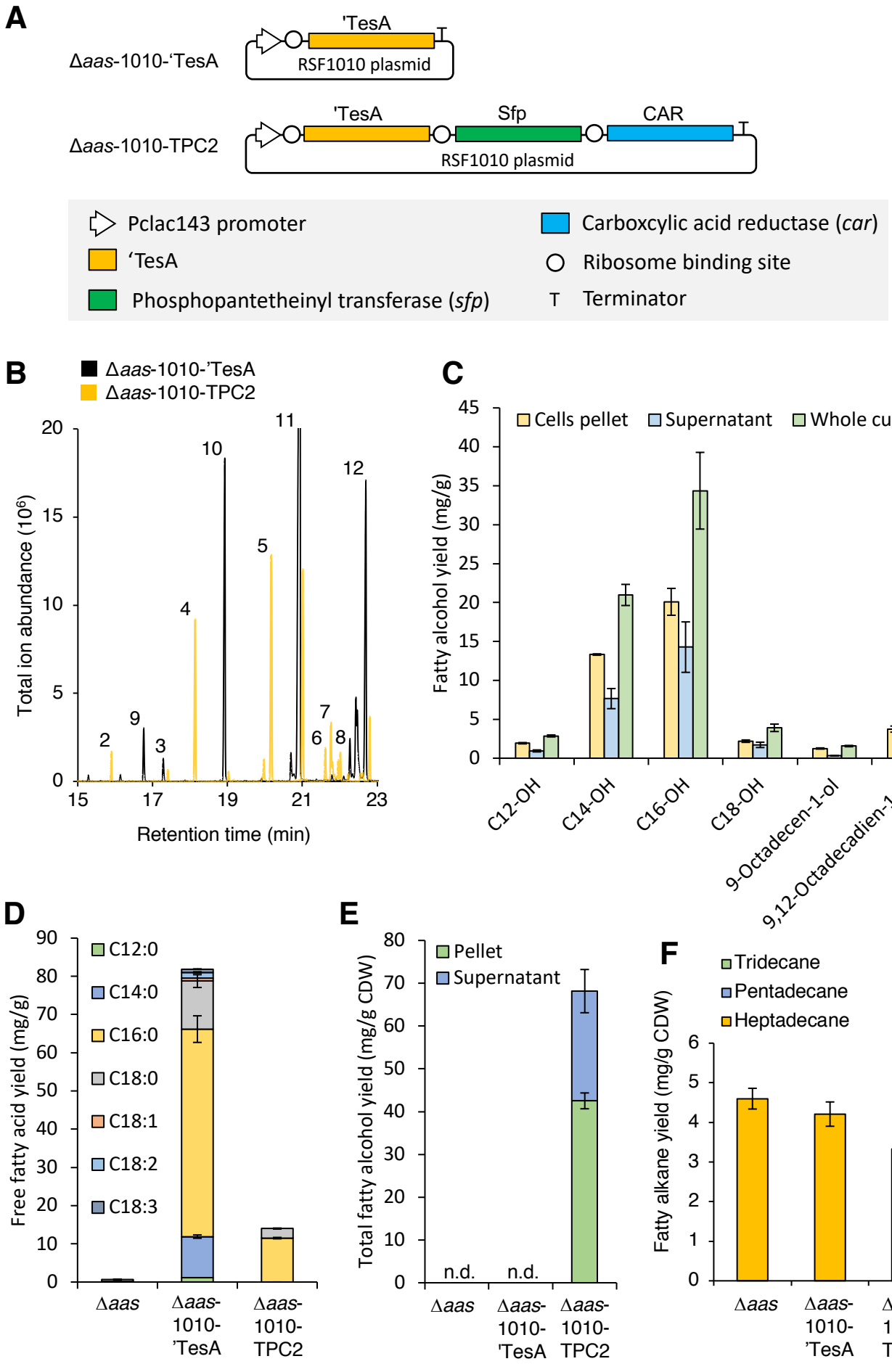
A
Δaas-1010-'TesA
'TesA
RSF1010 plasmid
Δaas-1010-TPC2
'TesA
Sfp
CAR
RSF1010 plasmid
Pclac143 promoter
'TesA
Phosphopantetheinyl transferase (sfp)
Carboxcylic acid reductase (car)
Ribosome binding site
T Terminator
B
Δaas-1010-'TesA
Δaas-1010-TPC2
Total ion abundance (10^6)
Retention time (min)
C
Cells pellet
Supernatant
Whole culture
Fatty alcohol yield (mg/g)
C12-OH
C14-OH
C16-OH
C18-OH
9-Octadecen-1-ol
9,12-Octadecadien-1-ol
D
C12:0
C14:0
C16:0
C18:0
C18:1
C18:2
C18:3
Free fatty acid yield (mg/g)
Δaas
Δaas-1010-'TesA
Δaas-1010-TPC2
E
Pellet
Supernatant
Total fatty alcohol yield (mg/g CDW)
n.d.
n.d.
Δaas
Δaas-1010-'TesA
Δaas-1010-TPC2
F
Tridecane
Pentadecane
Heptadecane
Fatty alkane yield (mg/g CDW)
Δaas
Δaas-1010-'TesA
Δaas-1010-TPC2

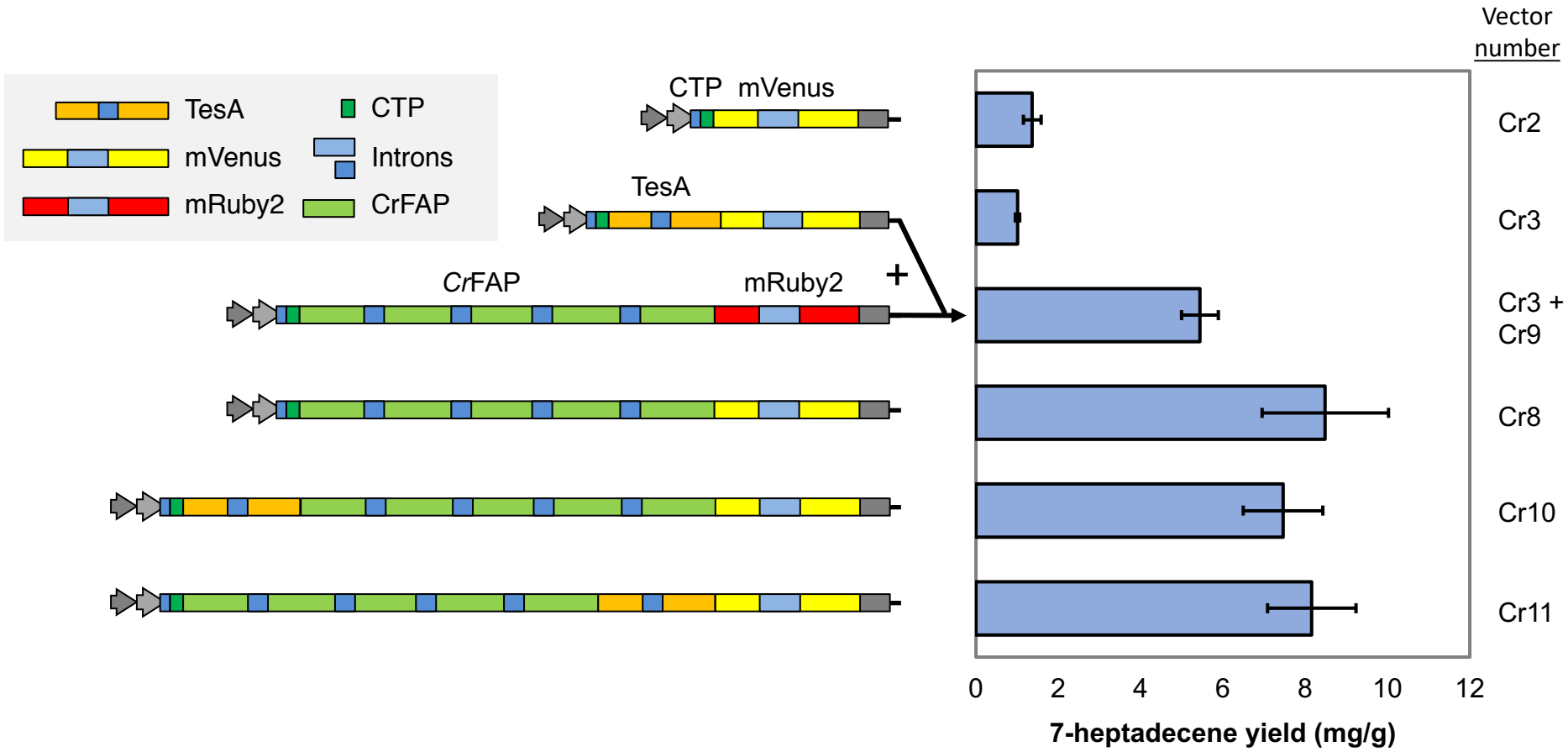
TesA
mVenus
mRuby2
CTP
Introns
CrFAP
CTP mVenus
TesA
CrFAP
mRuby2
+
Vector number
Cr2
Cr3
Cr3 + Cr9
Cr8
Cr10
Cr11
0
2
4
6
8
10
12
7-heptadecene yield (mg/g)

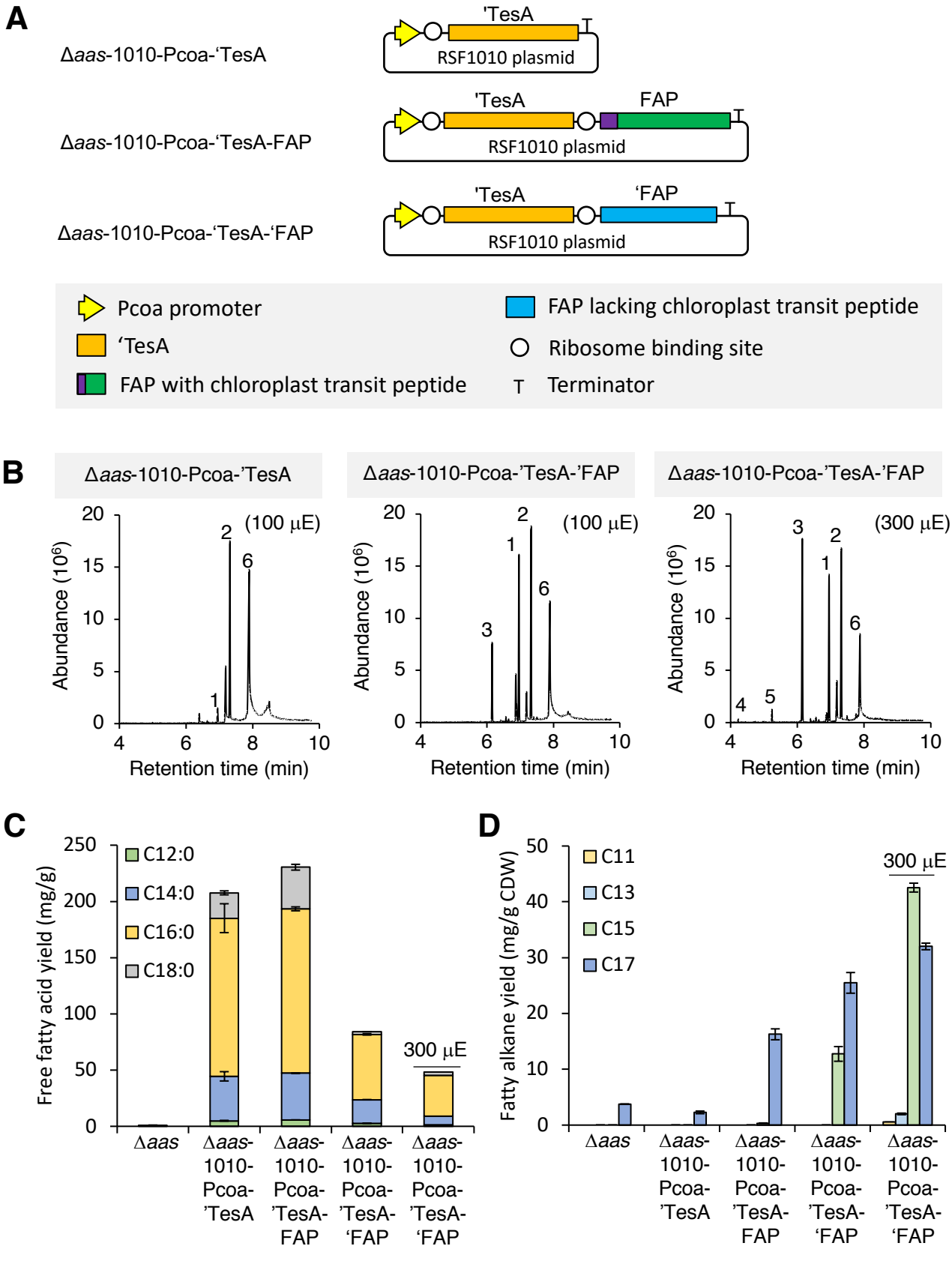
A
Δaas-1010-Pcoa-'TesA
'TesA
RSF1010 plasmid
Δaas-1010-Pcoa-'TesA-FAP
'TesA
FAP
RSF1010 plasmid
Δaas-1010-Pcoa-'TesA-'FAP
'TesA
'FAP
RSF1010 plasmid
Pcoa promoter
'TesA
FAP with chloroplast transit peptide
FAP lacking chloroplast transit peptide
Ribosome binding site
T Terminator
B
Δaas-1010-Pcoa-'TesA
Δaas-1010-Pcoa-'TesA-'FAP
Δaas-1010-Pcoa-'TesA-'FAP
(100 μE)
(100 μE)
(300 μE)
Abundance (10^6)
Retention time (min)
C
Free fatty acid yield (mg/g)
C12:0
C14:0
C16:0
C18:0
300 μE
Δaas
Δaas-1010-Pcoa-'TesA
Δaas-1010-Pcoa-'TesA-FAP
Δaas-1010-Pcoa-'TesA-'FAP
Δaas-1010-Pcoa-'TesA-'FAP
D
Fatty alkane yield (mg/g CDW)
C11
C13
C15
C17
300 μE
Δaas
Δaas-1010-Pcoa-'TesA
Δaas-1010-Pcoa-'TesA-FAP
Δaas-1010-Pcoa-'TesA-'FAP
Δaas-1010-Pcoa-'TesA-'FAP